Available online at www.sciencedirect.com
SCIENCE DIRECT®
PERGAMON
Continental Shelf Research 23 (2003) 513–532
CONTINENTAL SHELF RESEARCH
www.elsevier.com/locate/csr

Video observations of nearshore bar behaviour. Part 2: alongshore non-uniform variability

I.M.J. van Enckevort[a,*], B.G. Ruessink[b,1]

[a] Department of Physical Geography, IMAU, Utrecht University, P.O. Box 80115, 3508 TC Utrecht, Netherlands
[b] WL|Delft Hydraulics, Marine and Coastal Management, P.O. Box 177, 2600 MH Delft, Netherlands

Received 19 November 2001; received in revised form 17 June 2002; accepted 9 December 2002

Abstract

A considerable portion of the variability in nearshore sandbars is related to changes in the plan shape of quasi-rhythmic alongshore non-uniform features, such as rip channels and crescentic shapes. These changes may include changes in their alongshore length, cross-shore amplitude and alongshore position. Here, we use complex empirical orthogonal eigenfunction analysis to quantify these changes from a 3.4-year data set of almost daily time-exposure images of the double-barred coast at Noordwijk (Netherlands).

The observed alongshore non-uniform features had alongshore lengths between 380 and approximately 3000 m and lifetimes in the order of months, considerably longer than the characteristic time scale of individual wave events. Transitions from one feature to another were mostly gradual, resulting from an alongshore differential growth in amplitude. Abrupt transitions, that is, the existing features disappeared entirely and were subsequently replaced by different features, were barely observed and did not always take place during high-energy wave events. The amplitude of the non-uniform features varied between 0 and 30 m on a weekly to monthly scale, unrelated to variations in the wave height. In addition, the features migrated back and forth along the shore with typical rates of O(10 m/day) on weekly scales with the rates increasing with an increase in the alongshore component of the wave power. On the whole our observations suggest that alongshore non-uniform sandbar variability is governed by free behaviour rather than by the direct forcing of the prevailing wave conditions.

Keywords: Nearshore bars; Rhythmic features; Alongshore bar migration; Time scales; Video imagery

1. Introduction

Nearshore bars, common subtidal features along most of the world's sandy coastlines, are generally oriented shore parallel, but also contain quasi-rhythmic alongshore non-uniformities often referred to as three-dimensional (3-D) features. Examples hereof are rip channels, characterised by narrow seaward perturbations in otherwise straight bars (e.g., Fig. 1a), and crescentic plan

*Corresponding author. Tel.: +31-30-2532982; fax: +31-30-2531145.
E-mail address: i.vanenckevort@geog.uu.nl (I.M.J. van Enckevort).
[1] Now at: Department of Physical Geography, IMAU, Utrecht University, P.O. Box 80115, 3508 TC Utrecht, Netherlands.

0278-4343/03/$ - see front matter
doi:10.1016/S0278-4343(02)00235-2

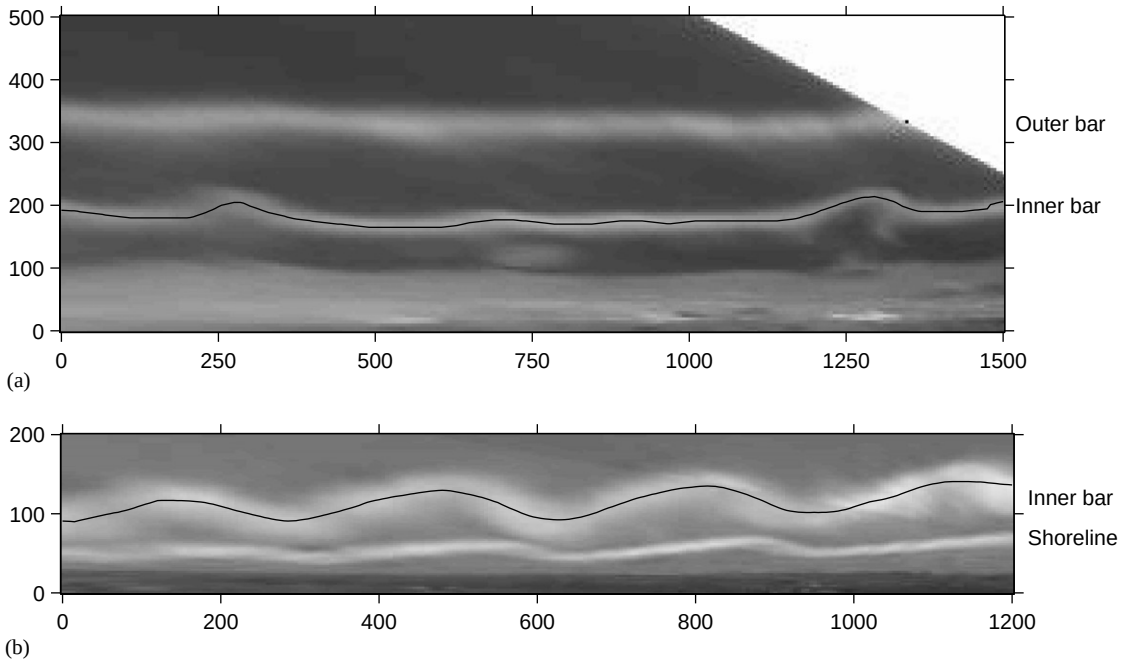

Fig. 1. Time-exposure video images showing examples of alongshore non-uniformities in nearshore bars. In the images, the white bands are caused by persistent wave breaking and reflect the location of the underlying sandbar. In (a) the inner bar is intersected by rather narrow seaward perturbations, characteristic of the presence of rip channels. In (b) the bar shows almost rhythmic sinusoidal variations, referred to as crescentic plan shapes. Image (a) is from Noordwijk, Netherlands, image (b) from Duck, NC, USA. The black lines in the inner-bar intensity bands are the computed bar crest lines, see Section 2. All axes are in m.

shapes (e.g., Fig. 1b). Changes in these non-uniformities, for instance related to their growth or decay, or their alongshore position, may make up a considerable portion of the natural variability of nearshore bars, particular on time scales of a few months or less (e.g., Sonu and Russell, 1966; Sallenger et al., 1985; Ruessink et al., 2000; Van Enckevort and Ruessink, 2001). Yet, the evolution of non-uniformities in nearshore bars is poorly understood.

Non-uniformities in nearshore bars have traditionally been classified into discrete states, including crescentic bars and transverse bars with rips (Wright and Short, 1984; Lippmann and Holman, 1990). The observations on which these 'state models' are based show that, generally, bars are linear during high-wave conditions and gradually develop non-uniformities during subsequent low-wave conditions. The straightening of bars is often abrupt, occurring during a single storm event, whereas the development of non-uniformities is typically sequential with increasing alongshore variability over time. Lippmann and Holman (1990) observed that mature crescentic features evolve some 5–7 days after large-wave events and Wright et al. (1985) observed a periodicity of 15–20 days in the bar state time series, attributed to the passage of low-pressure weather systems. Bar state models are qualitative in nature, and do not include (changes in) quantitative measures of the non-uniformities, such as their alongshore wavelength L, defined as the alongshore recurrence interval of the feature (e.g. rip spacing), or their cross-shore amplitude A, defined as half the distance between the most seaward and the most shoreward position of the feature.

Table 1 presents an overview of values of the alongshore length, cross-shore amplitude and alongshore migration rate of non-uniformities as compiled from the literature. This overview

Table 1
Overview observed non-uniform bar morphology and alongshore migration

Site	Geomorphology			Hydrodynamics		Data set		Characteristics non-uniformities			Reference
	Setting	Sediment (μm)	Slope[a] $1/\beta$	Tides (m)	Waves[b]	Region	Resolution	A (m)	L (m)	c_m (m/day)	
Rips											
Narrabean beach, Australia	Pocket	250–500	30	1.3–1.6	Both	Subtidal	Daily (19 months)		170–500	10–40	Short (1985)
Palm beach, Australia	Pocket	3000	50	1.6	Both	Subtidal	Daily (23 months)		≈100	0–20	Ranasinghe et al. (1999)
Muriwai, New Zealand	Straight	<250	100	4.0	Both	Subtidal	2 in 2 weeks		365–750		Brander et al. (1999)
Terschelling, Netherlands	Straight	150–160	220	1.2–2.8	Sea	Inner bar	Yearly		700		Ruessink (1992)
Crescentic bars											
White Park Bay, Ireland	Pocket	Sand, shingle	100	1.8	Both	Inner bar	7–11 in 1 year		105–280		Carter and Kitcher (1979)
White Park Bay, Ireland	Pocket	Sand, shingle	100	1.8	Both	Outer bar	6 in 1 year		200–450		Carter and Kitcher (1979)
Duck, NC, USA	Straight	180	80	1.0–1.3	Both	Single bar	4 in 2 weeks	20–30	≈300	20	Sallenger et al. (1985)
Kouchibouguac Bay, Canada	Straight	Sand	200	0.4–1.3	Sea	Outer bar	20 in 2 years	18–68	288–1232	0.3	Greenwood and D-A (1975)
Various coasts, Japan						Subtidal	≈ yearly		40–1000		Homma and Sonu (1962)
Mediterranean coast, Israel	Straight	Sand	100	0.3–0.6	Sea	Subtidal	Few per year		175–300		Bowman and Goldsmith (1983)
Alexandria, Egypt	Straight	130–1600	20–30		Sea	Subtidal	Once		≈100		Nafaa and Omran (1993)
Cape-Ferret, France	Straight	250–500	70	4.5	Both	Subtidal			500–1000		Froidefond et al. (1990)
Hald beach, Denmark	Straight	145		0.4	Sea	Inner	12 in 6 months		30–130		Aagaard (1988)
Various coasts, Denmark			40–170	0.3–0.4	Sea	Subtidal	≈ yearly		30–980		Aagaard (1989)
Terschelling, Netherlands	Straight	150–160	220	1.2–2.8	Sea	Middle bar	Yearly		1500–3000		Ruessink (1992)
Holland coast, Netherlands	Straight	150–200	120–150	1.2–1.9	Sea	Inner bar	Yearly		341–984	0.2	Short (1992)[c]
Holland coast, Netherlands	Straight	150–200	120–150	1.2–1.9	Sea	Outer bar	Yearly		1000–3000		Wijnberg (1995)
Egmond, Netherlands	Straight	150–200	120	1.3–1.6	Sea	Inner bar	Once		250		Wolf (1994)
Egmond, Netherlands	Straight	150–200	120	1.3–1.6	Sea	Inner bar	30 in 6 weeks	5–40	575	0–150	Ruessink et al. (2000)

[a] β is the mean slope of the nearshore area, preferably of the bar region only.
[b] sea, swell, or both sea and swell.
[c] Short (1992) named all non-uniform features rips, but, according to the present author, most observed non-uniform features were crescentic bars.

indicates that L, generally, is O(100−1000 m) with larger values for the outer than for the inner bar. Amplitudes have only occasionally been measured and reported values range from 5 to ≈70 m. The non-uniform features have often been observed to migrate along the coast with rates of O(10 m/day), presumably driven by the alongshore current (e.g., Ruessink et al., 2000). However, these quantitative descriptions listed in Table 1 are limited to data sets with a poor temporal resolution or with a duration of a few weeks at most. Therefore, the temporal evolution of non-uniform features, in particular regarding their length, amplitude and alongshore position, is still poorly understood.

This paper is part 2 of a two-part study on nearshore bar behaviour determined from video imagery and focuses on its alongshore non-uniform component. Part 1 (Van Enckevort and Ruessink, 2003, henceforth referred to as Part 1) focuses on its alongshore uniform component, that is on/offshore bar migration. The objectives of the present paper are (1) to describe the temporal evolution of non-uniform features in particular considering changes in L, A and c_m and (2) to link this evolution to the obvious potential wave forcing. These objectives are pursued using the same data set as in Part 1, a 3.4-year data set of almost daily, video-based bar crest observations collected at the double barred coast at Noordwijk, Netherlands. A brief description hereof is provided in Section 2. In contrast to the data sets listed in Table 1, the present data set combines a high temporal resolution with a long duration. The temporal evolution of the observed non-uniform features, quantified using complex empirical orthogonal function analysis (Section 3), is described in Section 4 using time series of L, A and c_m. In contrast to the analyses in Part 1, the evolution is not described at particular predefined time scales (as there is no consensus in the literature on what the dominant scales would be). Instead, quantification of the time scales for the evolution is one of the outcomes of the present research. The link between changes in L, A and c_m, and offshore wave forcing is investigated in Section 5. Our main findings are discussed and summarised in Section 6.

2. Data set

Oblique 10-minute time-exposure video images were collected automatically every daylight hour at the double-barred beach at Noordwijk, Netherlands from March 1995 to September 1998. The digital camera was equipped with a 12.5-mm lens and was mounted on the roof of a hotel at about 60 m above mean sea level. For the present work, a single high-quality image was selected per day, see Part 1 for further information. The selected images were transformed to a 5×5 m grid, examples of which are given in Fig. 1. The rectified images extend 1.2 km in the cross-shore (x) and 3 km in the alongshore (y) direction, and have a spatial resolution in the bar area of about 4–20 m in the cross-shore and 10–100 m in the alongshore direction, with the higher values farther away from the camera. Subsequently, the bar crest location was computed by sampling the cross-shore location of the image intensity peaks alongshore (see Part 1), see Fig. 1 for examples. In this way, a matrix $X(t, y)$ was constructed, consisting of bar crest locations X at times t and alongshore locations y. In total, the inner bar crest was sampled 632 times over 2300 m, whereas the outer bar location was sampled 391 times over 2000 m. This means that, on average, the inner bar was measured every other day, whereas the outer bar was measured approximately once every 3 days. However, the time interval between subsequent observations was irregular, with long intervals during low-energetic periods without wave breaking. Only 5% of these intervals were larger than 10 days.

The bar crest matrix $X(t, y)$ describes both the alongshore uniform bar crest morphology, expressed by the alongshore averaged cross-shore bar crest location $X_y(t)$ and analysed in Part 1, and the alongshore non-uniform bar crest morphology $D(t, y)$, computed as the deviations from the alongshore averaged bar position

$$D(t, y) = X(t, y) - X_y(t). \quad (1)$$

The deviation lines $D(t, y)$ are shown in Figs. 2 and 3 for the outer and the inner bar, respectively. In these figures, the deviation lines are vertically stacked with warm (cold) colours corresponding to

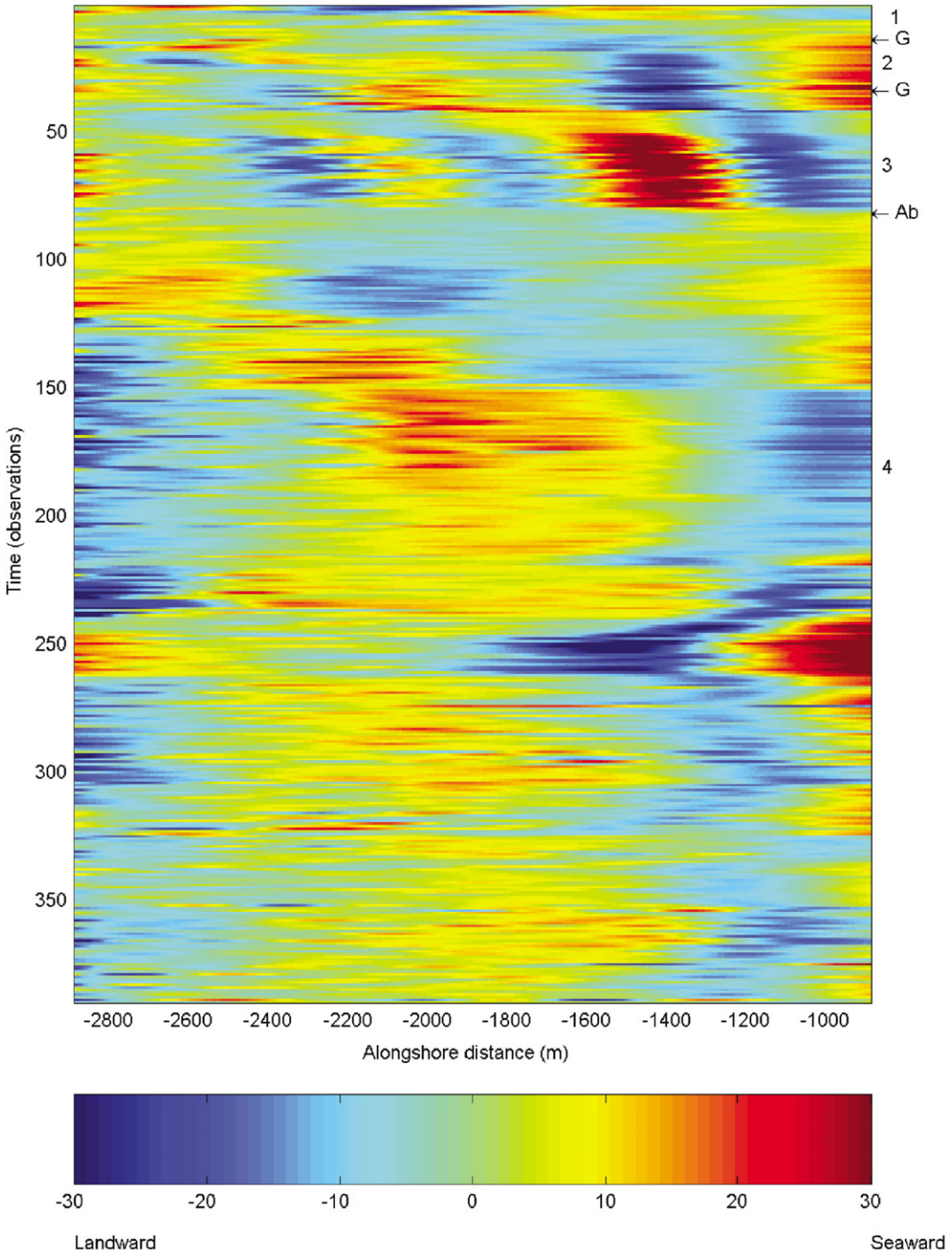

Fig. 2. Time stack of alongshore deviation lines for the outer bar. The numbers 1–4 correspond to the numbering of the non-uniform features listed in Table 2. Arrows indicate class transitions. Class transitions marked with 'Ab' are abrupt, whereas those marked with 'G' are gradual. For further explanation see text.

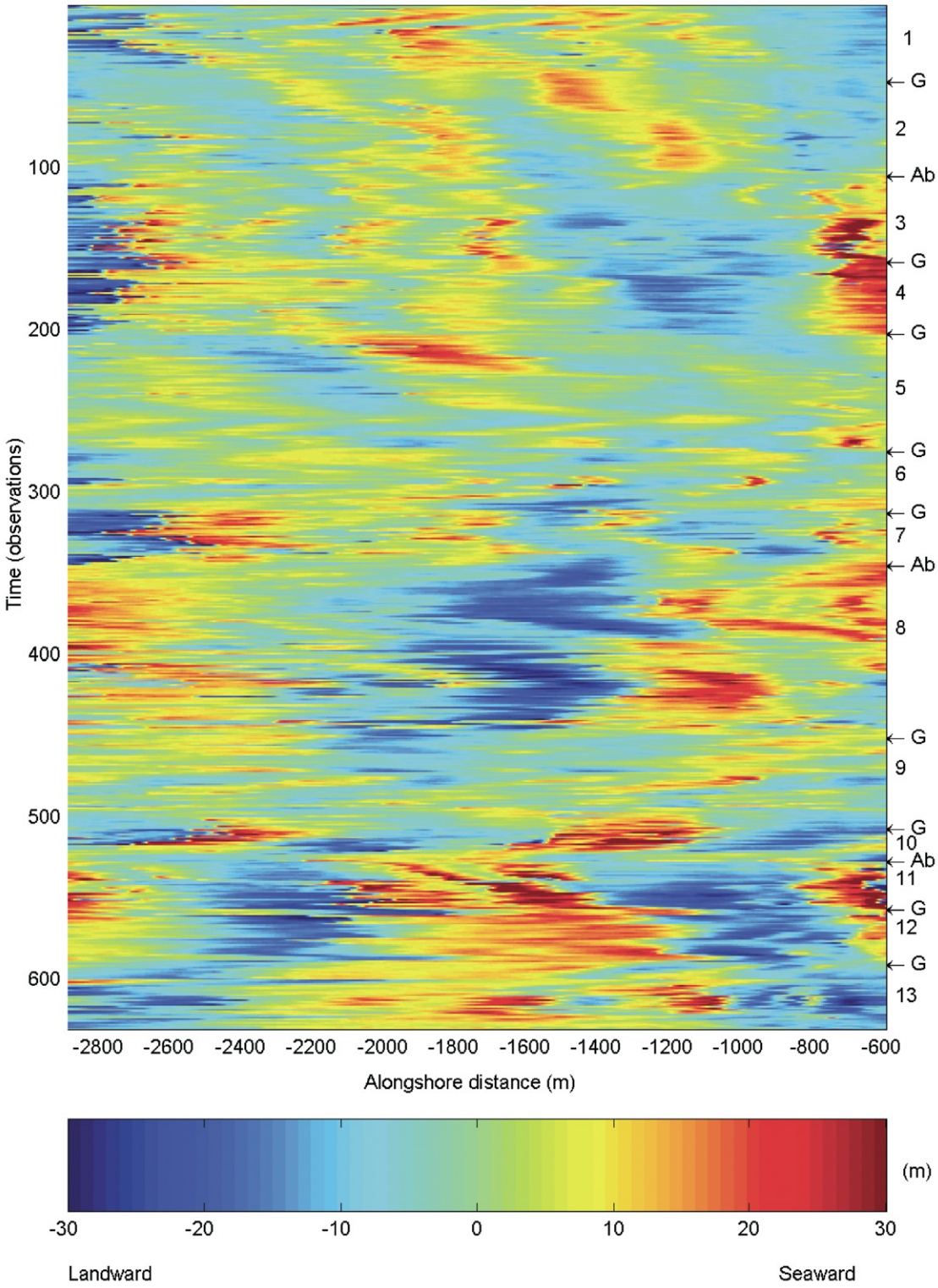
Time (observations)
100
200
300
400
500
600
1
← G
2
← Ab
3
← G
4
← G
5
← G
6
← G
7
← Ab
8
← G
9
← G
10
← Ab
11
← G
12
← G
13
-2800 -2600 -2400 -2200 -2000 -1800 -1600 -1400 -1200 -1000 -800 -600
Alongshore distance (m)
(m)
-30 -20 -10 0 10 20 30
Landward
Seaward

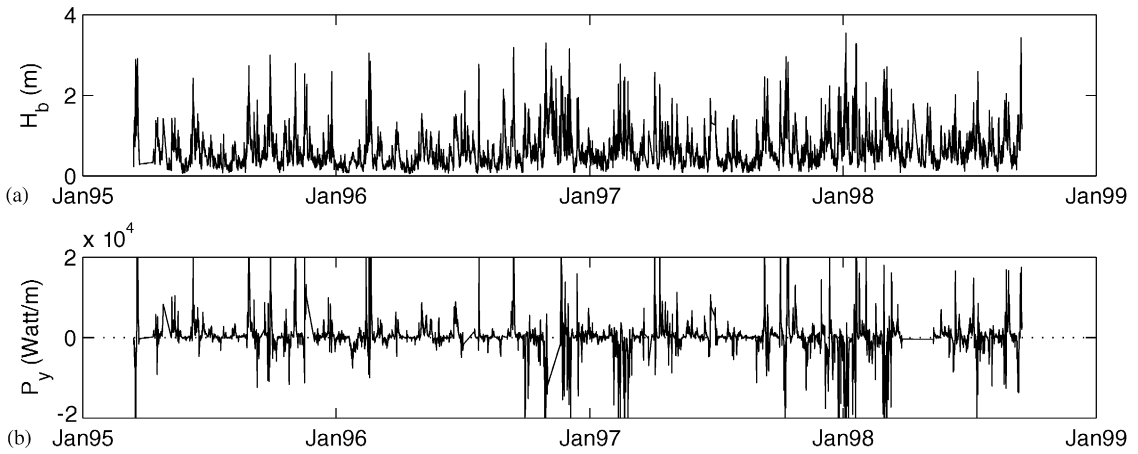

Fig. 4. Time series of (a) H_b and (b) P_{y0}.

seaward (landward) deviations. Thus, non-uniform features like crescentic bars are displayed by a horizontal alternation of warm and cold colours. Alongshore migration is reflected by a vertical displacement in the location of the colour bands.

Offshore wave data (height, period and direction) were collected hourly by a directional wave buoy at IJmuiden in 21-m depth. For the purpose of the present study, the data were processed into two parameters that have been linked previously to the evolution of non-uniform features. The first parameter is the breaker height H_b. In the literature, linear bars have usually been associated with high-wave conditions, whereas non-linear bars have been associated with low-wave conditions (Wright and Short, 1984; Lippmann and Holman, 1990). Using linear wave theory and assuming that H_b is proportional to the water depth d ($H_b = \gamma d$, with $\gamma = 0.4$; Thornton and Guza, 1982), H_b is computed as

$$H_b = (H_{rms0}^2 c_{g0} \cos\theta_0)^{0.4} \left(\frac{\gamma}{g}\right)^{0.2}, \quad (2)$$

where H_{rms0} is the offshore root-mean-square wave height, c_{g0} is the deep water wave group velocity, θ_0 is offshore energy-weighted mean wave angle and g is the gravitational acceleration. c_{g0} is a function of the offshore wave period T_0. The second parameter is the alongshore component of the wave power P_{y0}, which may be used as a proxy of the alongshore current. Alongshore currents are often assumed to be the driving force for the alongshore migration of crescentic bars and rips (Ranasinghe et al., 1999; Ruessink et al., 2000). Following Komar (1998), P_{y0} was computed as

$$P_{y0} = \frac{\rho g^2}{32\pi} H_{rms0}^2 T_0 \sin\theta_0 \cos\theta_0, \quad (3)$$

where ρ is the sea water density ($=1025\ \mathrm{kg\,m^{-3}}$). H_b and P_{y0} both increase with H_{rms0}, but P_{y0} additionally reflects the angle of wave incidence with high values for obliquely incident waves. Time series of H_b and P_{y0} are shown in Fig. 4. The computed H_b with values between 0.1 and 3.5 m mainly varied on daily to weekly scales (Fig. 4a). P_{y0} was O(10^3 W/m) and varied on a daily to weekly scale as well (Fig. 4b). The high values of P_{y0} during storms reflect both the large wave height and the typical large angle of incidence. The tide at Noordwijk is semi-diurnal with a mean neap (spring) tidal range of 1.4 (1.8) m. During

Fig. 3. Time stack of alongshore deviation lines for the inner bar. The numbers 1–13 correspond to the numbering of the non-uniform features listed in Table 2. Arrows indicate class transitions. Class transitions marked with 'Ab' are abrupt, whereas those marked with 'G' are gradual. For further explanation see text.

storms water levels may increase by 1 m due to storm surges.

3. Method

The quantification of the alongshore length, cross-shore amplitude and alongshore migration rate of the non-uniform features in $D(t, y)$ requires an objective description of these features. The description can be considered as a form of feature extraction, for which, since its introduction in nearshore studies by Winant et al. (1975), empirical orthogonal function (EOF) analysis is routinely applied. The attempt in feature extraction is to associate the leading EOF modes with actual modes (in our cases, the non-uniform features) in the data. EOF analysis is limited to the detection of standing oscillations (Horel, 1984). Propagating features, visible in our data by the vertical displacement of colour bands in Figs. 2 and 3, are scattered in two or more modes (Wijnberg and Terwindt, 1995), which complicates their physical interpretation. A version of EOF known as complex EOF (CEOF) (Horel, 1984) appears to be better suited for the objective description of propagating features, as it can condense such features in a single mode. Following its extensive use in climate research (e.g., Rasmusson et al., 1981; Barnett, 1983; Horel, 1984), CEOF has recently been applied to coastal data as well (Liang and Seymour, 1991; Liang et al., 1992; Ruessink et al., 2000). Ruessink et al. (2000), for example, quantified the evolution of a crescentic bar during a six-week period, using CEOF analysis on bar crest lines. Note that we apply CEOF as a feature extraction technique, thereby separating non-uniform features from the ambient noise, and not, like Winant et al. (1975), to define 'generally valid' orthogonal functions.

In contrast to the data set analysed by Ruessink et al. (2000), our inner and outer bar data sets (Figs. 2 and 3) consist of a temporal succession of different non-uniform features. Because CEOF tends to describe domain-wide features (Merrifield and Guza, 1990), CEOF analysis of the entire inner and outer bar $D(t, y)$ will not be fruitful in describing L, A and c_m of individual features. Therefore, we decided to split up each $D(t, y)$ in a number of subsets using traditional classification techniques. Application of existing classification schemes (e.g., Wright and Short, 1984; Lippmann and Holman, 1990) was found to be largely non-discriminating (Van Enckevort, 2001), and, accordingly, we propose a division into the classes crescentic, undulating, irregular and rips (Fig. 5) based on the alongshore length scale and the regularity of the features in our data. Undulating features, defined as gentle features with a length scale larger than 2000 m, are the largest features (Fig. 5a). Irregular features (Fig. 5b) typically have lengths comparable to crescentic bars (Fig. 5c), but differ by their non-sinusoidal shape. Although rips may be remarkably regular, their distinguishing

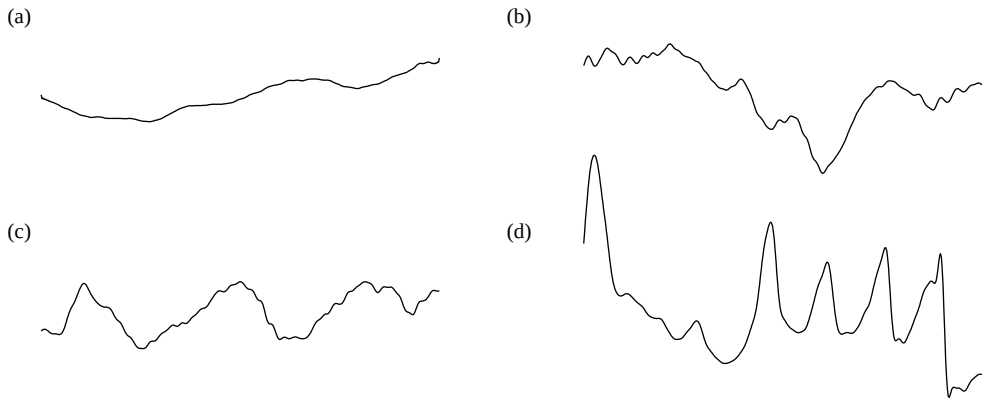

Fig. 5. Example bar crest lines of non-uniform features (a) undulating (b) irregular, (c) crescentic and (d) rips. Horizontal distance is 2300 m, vertical scale is about 20 times exaggerated. All features are displayed on the same scale.

characteristic is not their alongshore regularity, but the narrowness of the seaward protrusion (Fig. 5d). Linear bars were not classified separately, because bars are rarely completely linear, and the linearity is already expressed by A, with near-zero A for approximately linear features. CEOF analysis is now applied to the individual subsets.

The first step in the CEOF analysis was the transformation of the subset data matrix D into a complex data matrix D_c

$$D_c = D + \mathrm{i}\hat{D}, \tag{4}$$

where the real part is the original subset deviation matrix and the imaginary part is its Hilbert transform. The Hilbert transform was performed on each deviation line using a Fourier method: the amplitude of each spectral component is unchanged, but each component's phase is advanced by $\pi/2$. Then, the complex covariance matrix R was computed as

$$R = \frac{D_c^* D_c}{N_t}, \tag{5}$$

where * denotes the complex conjugate transpose and N_t is the number of deviation lines in a subset. R was subsequently decomposed into n_y real eigenvalues λ_n and spatial complex non-dimensional eigenvectors E_n. Here, n_y is the number of alongshore locations at which the deviation is sampled (i.e., 401 for the outer and 461 for the inner bar). The subscript n is an integer indicating the number of the ordered eigenvectors. The order is based on the amount of explained variance, expressed by the eigenvalue, with the first mode E_1 explaining most variance. The corresponding dimensional weightings w_n were obtained as

$$w_n = D_c E_n. \tag{6}$$

With the decomposition of D into the spatial pattern E_n and temporal weightings w_n, L, A and c_m can now be obtained. The alongshore wavelength L of the feature described by the nth eigenfunction was computed from the alongshore gradient in the unwrapped spatial phase θ_n as

$$L_n = 2\pi \frac{\Delta y}{\Delta \theta_n}, \tag{7}$$

with

$$\theta_n = \arctan\left[\frac{\Im\{E_n\}}{\Re\{E_n\}}\right], \tag{8}$$

where $\Im\{\,\}$ and $\Re\{\,\}$ denote the imaginary and real part, respectively. In Eq. (7), $\Delta y/\Delta\theta_n$ is computed from the best-fit linear line between θ_n and y, thus assuming a sinusoidal alongshore shape. The corresponding correlation coefficient r provides a measure of the validity of this assumption. A sinusoidal shape results in a constant $\Delta y/\Delta\theta_n$ and $r = 1$. Note that only a single L can be estimated for each subset, implying that temporal changes in L within a subset, should they exist, cannot be resolved. Time series of the cross-shore amplitude A of the feature described by the nth eigenfunction were computed from w_n as

$$A_n = [w_n w_n^*]^{1/2}. \tag{9}$$

Time series of the alongshore migration rate c_m were computed from L_n and the temporal phase ϕ_n as

$$c_m = \frac{L_n}{2\pi}\frac{\Delta\psi_n}{\Delta t}, \tag{10}$$

with

$$\psi_n = \arctan\left[\frac{\Im\{w_n\}}{\Re\{w_n\}}\right]. \tag{11}$$

In Eq. (10), Δt is the time step between two consecutive observations and $\Delta\psi_n$ is the corresponding temporal phase difference. A positive (negative) phase ramp implies that the feature described by the nth mode is propagating in the positive (negative) y direction. A more rigorous description of CEOF can be found elsewhere (e.g., Barnett, 1983; Horel, 1984; Von Storch and Zwiers, 1999).

4. Temporal evolution

Using our classification scheme, the data were classified into 13 subsets for the inner bar and 4 subsets for the outer bar (Table 2). Each subset, being a temporally continuous group bounded by class transitions, contained the evolution of a single non-uniform feature. The inner bar features

Table 2
Classification non-uniform bar shape

	Start date (day-month-year)	End date (day-month-year)	Alongshore shape	T (days)
Outer bar				
1	15-03-1995	29-03-1995	Undulating with crescentic	14
2	30-03-1995	24-04-1995	Undulating	25
3	25-04-1995	28-08-1995	Crescentic	125
4	29-08-1995	16-09-1998	Undulating	1114
Inner bar				
1	15-03-1995	17-05-1995	Undulating with rips	63
2	18-05-1995	28-08-1995	Crescentic	102
3	29-08-1995	02-11-1995	Rips	65
4	03-11-1995	13-02-1996	Irregular	102
5	14-02-1996	16-07-1996	Undulating with crescentic	153
6	11-09-1996	09-11-1996	Undulating with rips	59
7	14-11-1996	08-02-1997	Irregular	86
8	09-02-1997	11-10-1997	Irregular with crescentic	244
9	07-11-1997	01-02-1998	Undulating with crescentic	86
10	02-02-1998	09-03-1998	Crescentic	35
11	10-03-1998	02-05-1998	Irregular	53
12	04-05-1998	12-07-1998	Crescentic	69
13	13-07-1998	16-09-1998	Irregular	65
Averages for outer and inner bar data set				
			Undulating	216
			Irregular	110
			Crescentic	104
			Rips	62

could be any of the four classes with occasionally, rips and crescentic features superimposed on larger scale irregular or undulating features. The outer bar features were classified as undulating and crescentic only. In one subset, a crescentic feature was superimposed on a larger scale undulating feature. Typical rip morphologies were never observed in the outer bar. Each non-uniform feature is numbered and listed in Table 2. Most class transitions were gradual (transitions indicated with G on the right-hand side of Figs. 2 and 3). Usually, some seaward protrusions grew, whereas others disappeared, an example of which is shown in Fig. 6. In this way, the alongshore length scale or the alongshore regularity changed gradually, eventually resulting in another class. Other class transitions were abrupt (transitions indicated with Ab on the right-hand side of Figs. 2 and 3). In these cases, existing protrusions disappeared from one observation to the other, and, subsequently, a completely new set of seaward and landward protrusions developed, with another alongshore shape or another alongshore length scale. Such changes are here defined as a morphological reset.

The first complex eigenfunction described the main non-uniform feature in each subset well, explaining 46–84% of the total variance. When present, superimposed non-uniform features were described by the second complex eigenfunction, which explained an additional 18–28% of the variance in the subsets. Reconstructed deviation lines, using the first mode (or the first two for superimposed features) resemble the original deviation data well (compare Figs. 3 and 7). The evolution of each feature was then quantified by temporal changes in L, A and c_m. The results in the following may be affected by our classification of the individual subsets which is to some extent subjective. Subjectivity mainly affects the begin

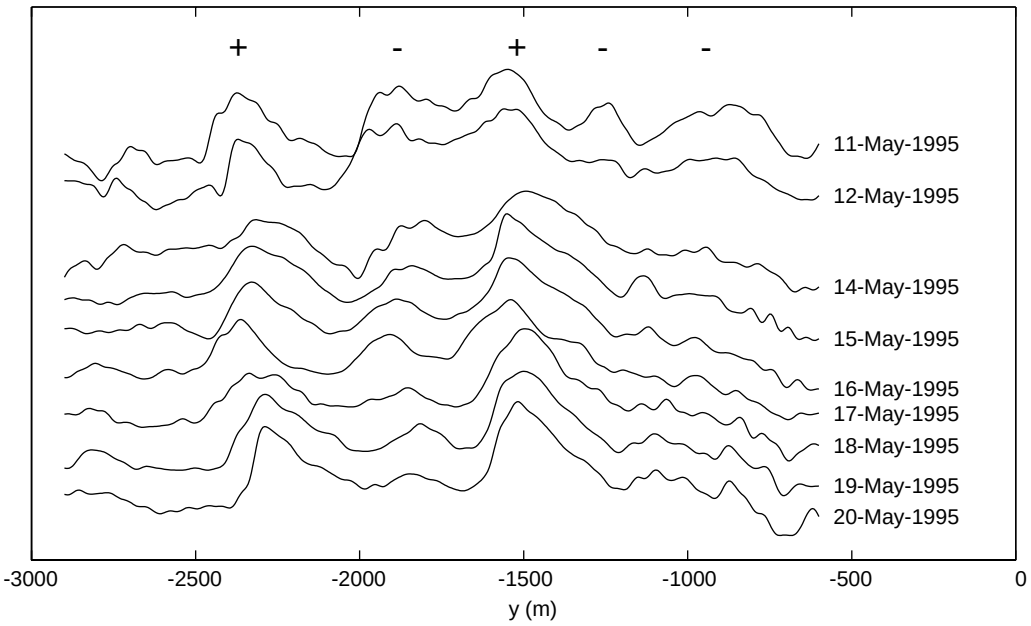

Fig. 6. Sequence of barlines showing gradual change in L. Time increases from top to bottom. Protrusion indicated with + grow in time, whereas protrusion indicated with − gradually disappear. Maximum cross-shore amplitudes are ≈30 m.

and end dates of the subsets, especially in case of gradual class transitions. But the effect on the further quantification will be limited, as the changes mainly took place within several days to a few weeks, whereas the features subsequently remained present for several months (Figs. 2 and 3). Applying CEOF to slightly different subsets did not result in significantly (given the spatial accuracy of the data, see Section 2) different values for L, A and c_m.

4.1. Alongshore length

For each of the 13 inner and 4 outer bar features, a domain-wide value for the alongshore length L was computed using Eq. (7). As shown in Table 3, L varied between 380 and 2760 m. Note that CEOF even quantified the alongshore lengths of features that exceed the alongshore extent of the data set, being 2300 m for the inner and 2000 m for the outer bar (see Section 2). Probably, lengths up to ≈4 km (i.e., about twice the alongshore extent) may be quantified, although the lengths should be interpreted as approximate values (i.e., a value of 2760 m means ≈3 km instead of exactly 2760 m). Typically, rips were the smallest features with an average spacing of 430 m, followed by crescentic features with an average length of 990 m (Table 3). Irregular and undulating features had larger average lengths of 1850 and 2320 m, respectively (Table 3). The correlation coefficient r between unwrapped θ_1 (or θ_2) and y varied between 0.87 and 0.99, thus justifying the assumption of a sinusoidal shape used to compute domain-wide values for L. However, the fact that $r \neq 1$ suggests that most non-linear features were characterised by weak deviations from a regular sinusoidal shape, such as skewed crescents or an alongshore varying length. Residence times T, computed from the begin and end dates of all non-uniform features, varied between 14 and 1114 days (≈0.5–37 months) for the outer bar and between 35 and 244 days (≈1–8 months) for the inner bar (Table 2).

The data (see Figs. 2 and 3) indicate that changes in L during the lifetime of a feature (i.e., within a subset), which are unresolved by the CEOF analysis (see Section 3), were limited and mainly restricted to the initial development and final disappearance of non-uniform features during gradual class transitions. L then changed

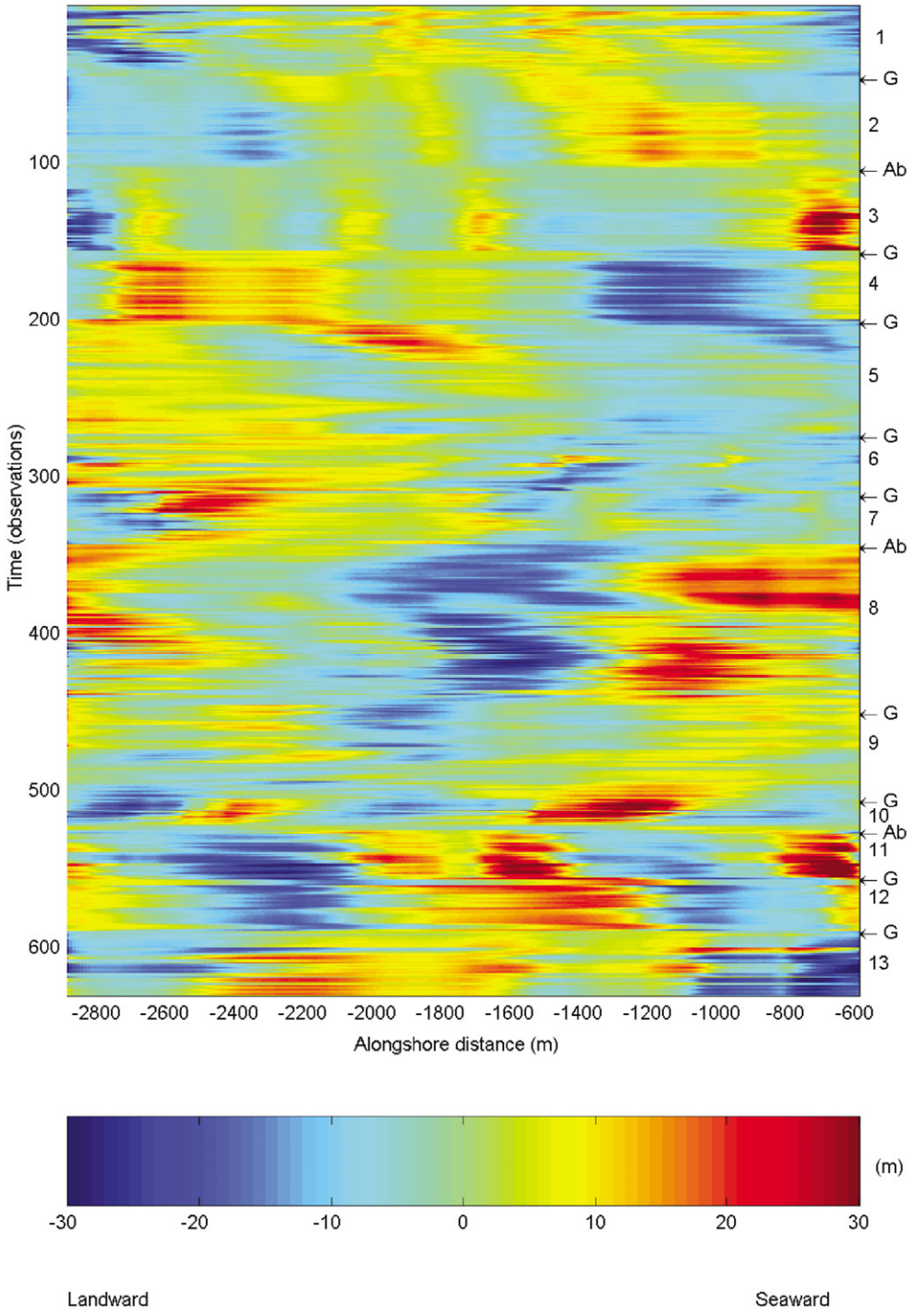

Fig. 7. Time stack of reconstructed alongshore deviation lines for the inner bar, similar to Fig. 3. Deviation lines are reconstructed using the first mode for features 2–4, 7, 10–13, and using the first two modes for features 1, 5, 6, 8 and 9.

Table 3
Overview descriptive morphological parameters for non-uniform features

	Alongshore shape	L (m)	A (m)
Outer bar			
1	Undulating with crescentic	2250 (1130)	20.2 (7.5)
2	Undulating	2730	14.8
3	Crescentic	970	14.9
4	Undulating	2230	13.0
Inner bar			
1	Undulating with rips	2760 (390)	8.8 (4.7)
2	Crescentic	960	9.2
3	Rips	380	8.6
4	Irregular	2370	13.9
5	Undulating with crescentic	2690 (870)	7.4 (5.7)
6	Undulating with rips	2460 (540)	9.0 (4.2)
7	Irregular	980	12.0
8	Irregular with crescentic	2140 (710)	13.5 (7.4)
9	Undulating with crescentic	2350 (850)	7.0 (4.7)
10	Crescentic	1070	14.0
11	Irregular	1210	18.3
12	Crescentic	1360	16.1
13	Irregular	2560	14.6
Averages for outer and inner bar data set			
	Undulating	2500	11.5
	Irregular	1850	14.4
	Crescentic	990	9.9
	Rips	430	5.8

Values between brackets refer to superimposed features.

O(100 m) on a weekly scale by differential grow in amplitude (see Fig. 6). During abrupt changes, L suddenly changed O(100−1000 m) from one dominant L to the subsequent dominant L, implying a full morphological reset of the system. In summary, L mainly varied O(100−1000 m) on a monthly time scale during class transitions. In addition, L changed O(100 m) on a weekly time scale, associated with alongshore differential grow in cross-shore amplitude.

4.2. Cross-shore amplitude

Time series of A, computed from the weightings on the first two eigenfunctions using Eq. (9), are displayed in Figs. 8 and 9 for the outer and inner bar, respectively. At both bars, A varied between 1 m, representing approximately linear bars, and 30 m (Figs. 8 and 9). The larger changes in A mainly occurred on a monthly time scale and are partially bounded by class transitions. When bounded by class transitions, A was usually smallest near the class transition and largest between subsequent class transitions (e.g., inner bar feature 2), although the opposite pattern was observed as well (e.g., inner bar feature 5). Temporal minima in A during class transitions were mainly associated with abrupt class transitions. This drop in A may be interpreted as a morphological reset. Subsequently, new features developed causing A to increase again. Not all monthly changes were, however, associated with class transitions. Occasionally, A dropped momentarily to near-zero values in the middle of the feature's lifetime (e.g., inner bar feature 8). In addition to the monthly variations, A changed on a weekly time scale. The amplitudes of the main and superimposed features often changed simultaneously, although they may change independently as well. For example, in the beginning of 1997, the amplitude of the main non-uniform feature increased, while the amplitude of the superimposed feature remained constant.

4.3. Alongshore migration

Time series of c_m, computed from the temporal phase of the first two eigenfunctions using Eq. (10), are shown in Figs. 10 and 11 for the outer and inner bar, respectively. No systematic monthly changes in c_m were observed that were related to class transitions. Instead, c_m varied on a weekly scale between 0 and 185 m/day in the northward and 0 and 170 m/day in the southward direction (Figs. 10 and 11). Typically, c_m was O(10 m/day) in either northward or southward direction, with maximum rates around 150 m/day (Fig. 12). The migration rates at the inner bar were generally smaller than those at the outer bar (Fig. 12 and Table 4). Northward migration rates were typically larger than southward rates (Table 4), but occurred less frequently (Table 4). However, both the differences in magnitude and in frequency were small. The differences in migration rate for the different features were small (Table 4). Undulating features tended to migrate slightly

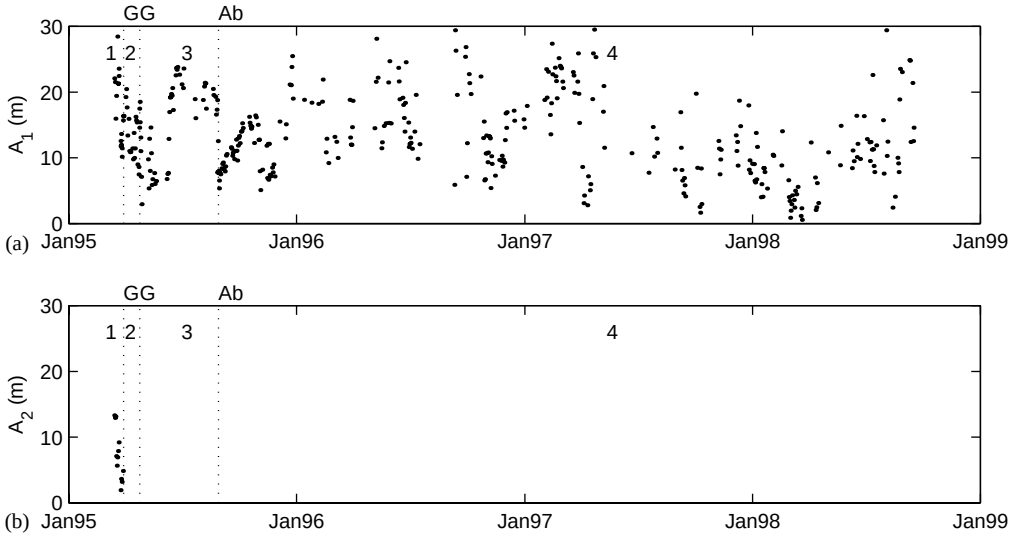

Fig. 8. Time series of the cross-shore amplitude for the outer bar based on the (a) first and (b) second eigenfunction. The numbers 1–4 correspond to the numbering of the non-uniform features listed in Table 2. Vertical dotted lines indicate the class transitions. Class transitions marked with 'Ab' are abrupt, whereas those marked with 'G' are gradual.

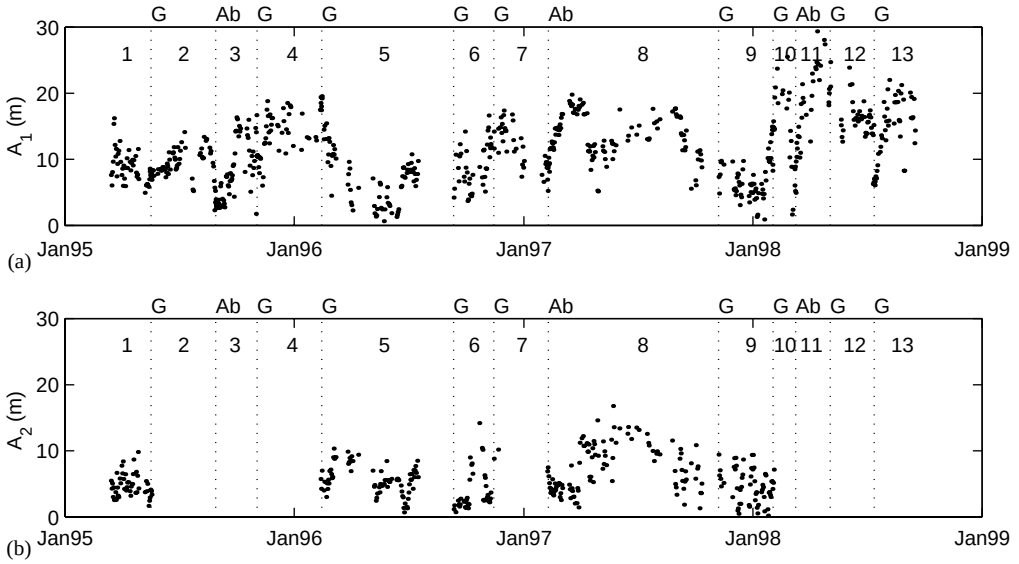

Fig. 9. Time series of the cross-shore amplitude for the inner bar based on the (a) first and (b) second eigenfunction. The numbers 1–13 correspond to the numbering of the non-uniform features listed in Table 2. Vertical dotted lines indicate the class transitions. Class transitions marked with 'Ab' are abrupt, whereas those marked with 'G' are gradual.

faster than irregular features, crescentic bars and rips. The rip migration rates seemed to be smaller than those for undulating, irregular and crescentic features, particularly the maximum rates (Table 4).

5. Forcing

In this section the relationship between the observed temporal variability in L, A and c_m and

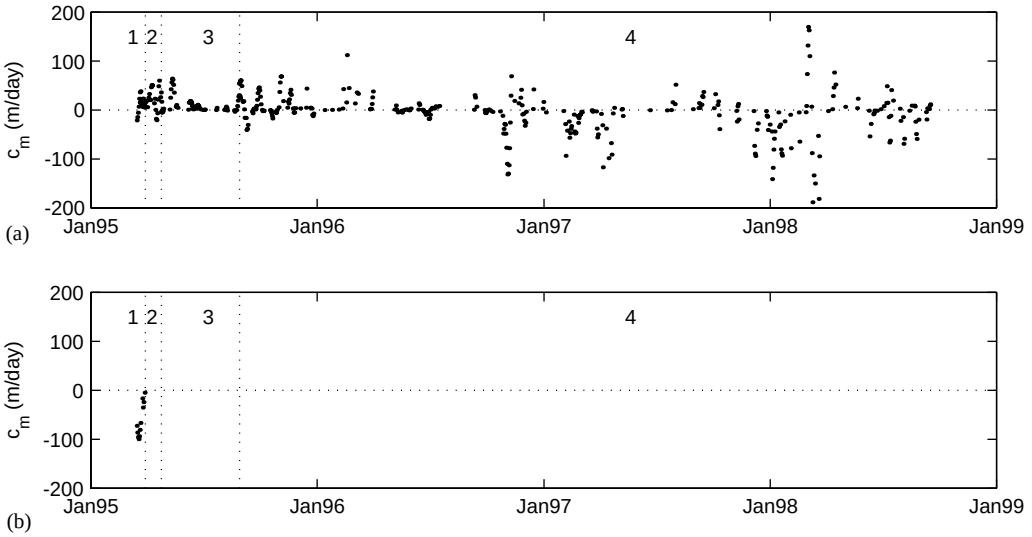

Fig. 10. Time series of the alongshore migration rate for the outer bar based on the (a) first and (b) second eigenfunction. The numbers 1–4 correspond to the numbering of the non-uniform features listed in Table 2. Vertical dotted lines indicate the class transitions.

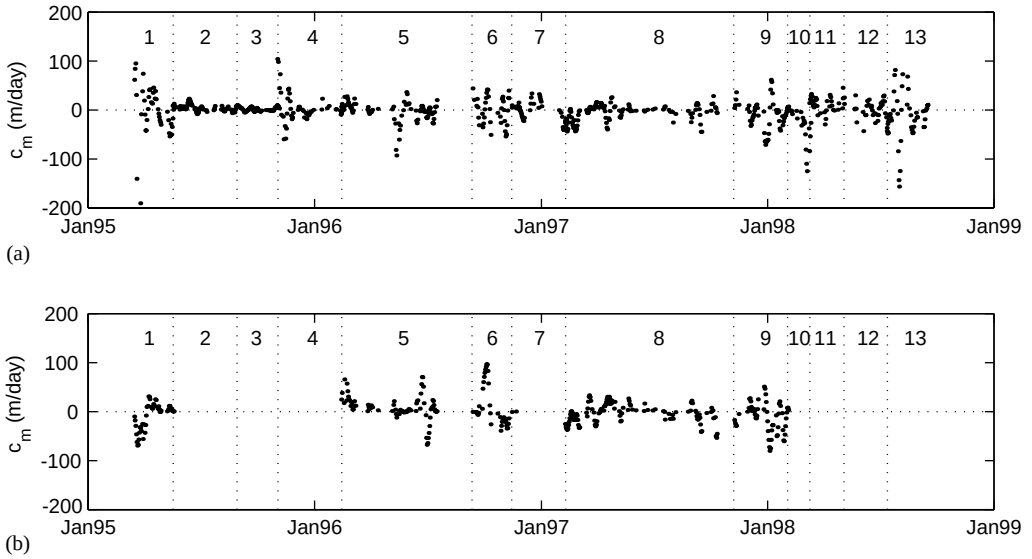

Fig. 11. Time series of the alongshore migration rate for the inner bar based on the (a) first and (b) second eigenfunction. The numbers 1–13 correspond to the numbering of the non-uniform features listed in Table 2. Vertical dotted lines indicate the class transitions.

the obvious potential forcing (H_b P_{y0}, see Section 2) is discussed. More specifically, the following three questions are addressed (1) During which conditions do the class transitions take place? (2) Is A coupled to H_b? (3) Is c_m coupled to P_{y0}?

As can be seen in Figs. 13 and 14, some class transitions were clearly associated with high-energetic ($H_b > 2$ m, or $P_{y0} > 2 \times 10^4$ W/m) periods (e.g., inner bar transitions 2–3 and 6–7). However, similar conditions occurred without

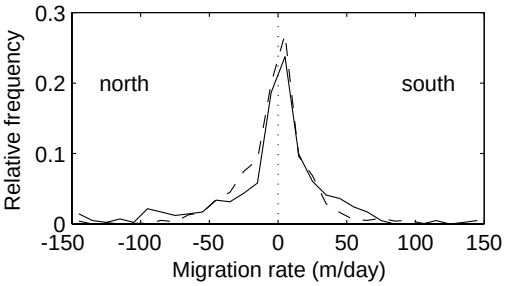

Fig. 12. Histograms of the northward and southward bar migration rate for the outer (drawn line) and inner (dashed line) bar.

class transition. Besides, class transitions were also observed during less energetic conditions (e.g., inner bar transition 1–2, $H_b < 1$ m and $P_{y0} \approx 0$ W/m). No systematic difference between abrupt and gradual transitions was observed.

For each value of A, a corresponding H_b was computed as the time average of all hourly H_b values since the previous observation of A. For some non-uniform features, A was found to decrease with increasing wave height (Fig. 15a), consistent with the transition to a linear bar in the state models of Wright and Short (1984) and

Table 4
Statistics of alongshore bar migration rates

	Northward migration (m/day)				Southward migration (m/day)			
	Mean	St. dev.	Max	N	Mean	St. dev.	Max	N
Outer bar	35	45	285	193	21	26	170	220
Inner bar	21	24	156	485	16	19	104	497
Undulating	31	40	285	282	21	24	170	280
Irregular	20	24	141	156	17	20	104	125
Crescentic	23	25	179	125	14	14	70	242
Rips	16	19	69	71	18	26	97	70

N is number of observations.

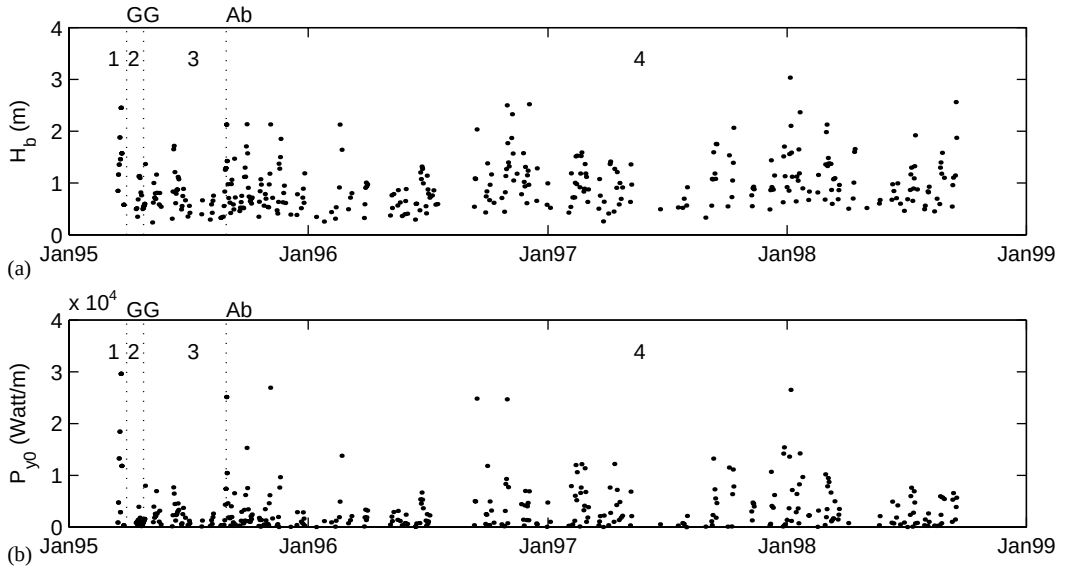

Fig. 13. Time series of (a) H_b and (b) P_{y0}, including the class transitions at the outer bar. The numbers 1–4 correspond to the numbering of non-uniform features listed in Table 2. Vertical dotted lines indicate the class transitions. Class transitions marked with 'Ab' are abrupt, whereas those marked with 'G' are gradual.

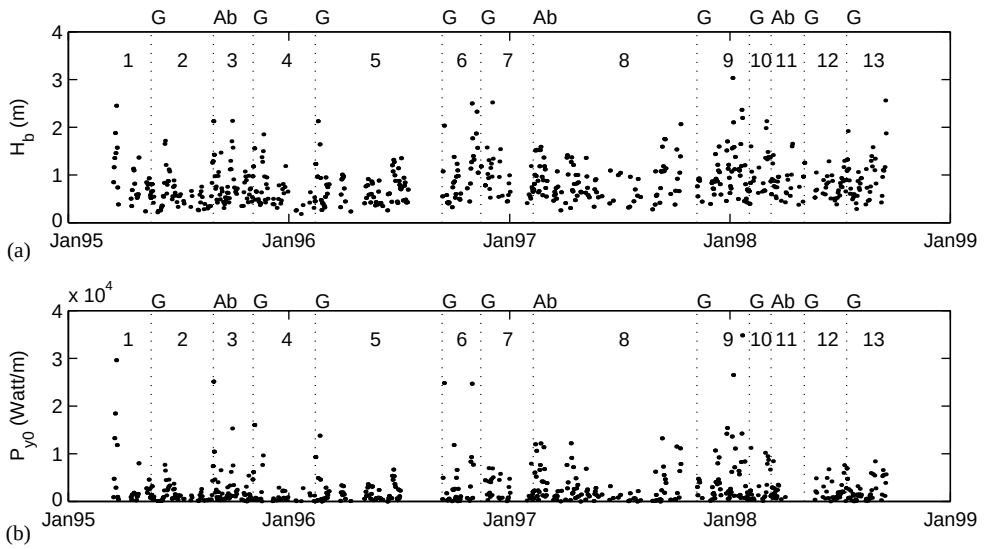

Fig. 14. Time series of (a) H_b and (b) P_{y0}, including the class transitions at the inner bar. The numbers 1–13 correspond to the numbering of non-uniform features listed in Table 2. Vertical dotted lines indicate the class transitions. Class transitions marked with 'Ab' are abrupt, whereas those marked with 'G' are gradual.

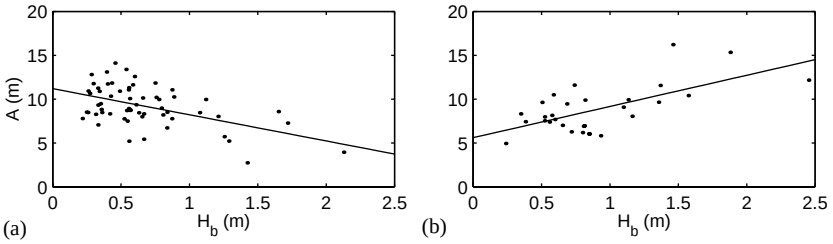

Fig. 15. Examples of the relation between cross-shore amplitude and wave height. Drawn line is the best-fit linear line. The relation in (a) is based on observations of inner bar feature 3 (crescentic; $r = -0.51$). The relation in (b) is based on observations of inner bar feature 2 (undulating; $r = 0.65$). Both relations are significant at the 95% level.

Lippmann and Holman (1990). However, opposite relations, i.e. increasing A with increasing wave height, were observed as well (Fig. 15b). Significant (at the 95% level) linear relations between A and H_b were found for undulating features, irregular features and crescentic bars, but not for rip morphologies. The relations were generally strongest for the undulating features (r^2 between 0.14 and 0.42), followed by crescentic bars (r^2 between 0.05 and 0.26). The relations for undulating features were, however, not consistent; the amplitude was observed to increase as well as to decrease with increasing wave height. For crescentic bars, the amplitude decreased with increasing wave height, whereas for irregular features the amplitude increased with increasing wave height. The positive relations were statistically different from the negative relations, but individual positive (or negative) relations were not statistically different at the 95% level. On the whole, the relation between A and H_b is unclear and inconsistent.

Generally, non-uniform features were found to migrate in the direction of P_{y0}, and the magnitude of c_m was found to increase linearly with the magnitude of P_{y0} (Fig. 16). For each feature, the relation between c_m and P_{y0} was described by the best-fit linear line between c_m and P_{y0}. Significant (at the 95% level) relations were found for all alongshore features. The relations were generally weakest for undulating features (r^2

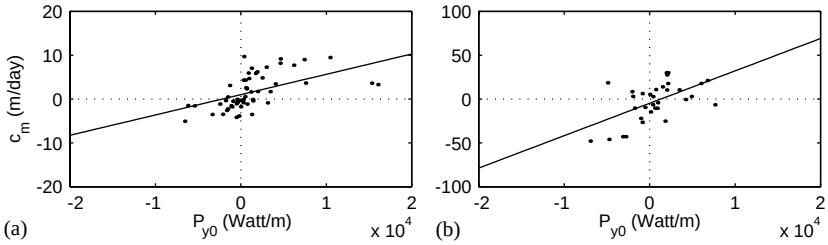

Fig. 16. Examples of the relation between alongshore migration c_m and the alongshore component of the offshore wave power P_{y0}. Drawn lines are the best-fit linear lines. The relation in (a) is based on observations of rips in the inner bar in September–October 1995 ($r = 0.60$). The relation in (b) is based on observations of the crescentic inner bar in May–July 1998 ($r = 0.55$).

between 0.04 and 0.17) and strongest for crescentic bars (r^2 between 0.06 and 0.34) and rips ($r^2 = 0.36$). Most relations were consistent and were in favour of the assumption that the alongshore migration is forced by the wave-driven alongshore current (see Section 2). Only two undulating features were observed to migrate against the direction of P_{y0}. The relations for rips and irregular features are not statistically different from the relations for crescentic bars.

6. Discussion and conclusions

The alongshore non-uniform bar morphology at Noordwijk (Netherlands) was quantified from a 3.4-year data set of almost daily, videoed bar crest lines, with the objectives (1) to describe the temporal evolution of alongshore non-uniform features and (2) to link this variability to the wave forcing, here expressed by the breaker height and the alongshore component of the wave power. The alongshore bar shape varied between the classes undulating, crescentic, irregular and rips, with alongshore lengths of 380 to approximately 3000 m. None of the features possessed a regular sinusoidal shape, but instead all features, were characterised by skewed crescents or an alongshore varying length. The observed class transitions were mostly gradual, resulting from an alongshore differential growth in amplitude of the features, and only occasionally abrupt, expressing a morphological reset. The features had lifetimes of 1–8 months in the inner bar and 0.5–37 months in the outer bar. These lifetimes contrast with the impression given in the literature that bars straighten during each high-wave event, implying a morphological reset every few days to several weeks (Wright et al., 1985; Lippmann and Holman, 1990). During their lifetime, the non-uniform features changed in amplitude between 0 and 30 m on a weekly to monthly scale. In addition, the non-uniform features migrated back and forth along the shore with typical rates of O(10 m/day) on weekly time scales.

Attempts to relate the changes in the morphological parameters to the wave forcing were inconclusive, except for the alongshore migration rate, which was significantly related to the alongshore component of the wave power, suggesting that the non-uniform features migrated alongshore under influence of the wave-driven alongshore current. The class transitions could not be associated with systematic changes in the breaker wave height or in the alongshore component of the wave power. Furthermore, no consistent linear relation between cross-shore amplitude and breaker wave height was observed. The general absence of consistent linear relations with the wave height and the alongshore component of the wave power raises the question whether this is because the link with forcing is more complex, or whether other wave parameters not investigated here (like wave steepness) are of importance, or whether it is the manifestation of free (i.e., non-forced) behaviour of a non-linear random system. In the most simple case of a forced response the morphology simply mirrors the forcing conditions, implying a linear relation between morphology and forcing, as investigated here. However, the link with the forcing may be more complex owing to non-linearities such as

response times depending on the wave conditions and response rates increasing with the degree of disequilibrium between the forcing and the antecedent morphology (Wright and Short, 1984). A more extensive analysis considering non-linear relations is needed to unravel the direct effect of wave forcing on the evolution of non-uniform features, should it exist. Alternatively, the nearshore bar system may be governed by free behaviour, implying that no direct relation, not even a complex one, between forcing and the evolution of non-uniform features exists. In this case, the system is dominated by non-linear feedback between forcing and response, resulting in self-organisational, potentially chaotic, behaviour (Southgate and Beltran, 1996; Coco et al., 2000). Our observations that the alongshore non-uniform features evolve gradually and thus have lifetimes that are long relative to the characteristic time scales of the wave forcing are consistent with the idea of strong morphologic feedback, and as such provide circumstantial evidence for free behaviour.

Acknowledgements

We would like to thank the staff of Grand Hotel 'Huis ter Duin' in Noordwijk for the permission to use the roof of their hotel as home for the ARGUS system and for their logistic support. Comments received on the Ph.D. thesis version of this paper from Huib de Swart, Giovanni Coco, Mark Davidson and Aart Kroon are greatly appreciated. This work was conducted as part of the EU-sponsored HUMOR project (contract EVK3-CT-2000-00037).

References

Aagaard, T., 1988. Nearshore bar morphology on the low-energy coast of northern Zealand, Denmark. Geografiska Annaler 70, 59–67.

Aagaard, T., 1989. Rhythmic beach and nearshore topography: examples from Denmark. Geografisk Tidsskrift 88, 55–60.

Barnett, T.P., 1983. Interaction of the monsoon and Pacific trade wind system at interannual time scales. Part I: the equatorial zone. Monthly Weather Review 111, 756–773.

Bowman, D., Goldsmith, V., 1983. Bar morphology of dissipative beaches: an empirical model. Marine Geology 51, 15–33.

Brander, R.W., Short, A.D., Osborne, P.D., Hughes, M.G., Mitchell, D.M., 1999. Field measurements of a large-scale rip-current system. In: Proceedings Coastal Sediments'99. ASCE, New York, pp. 562–575.

Carter, R.W.G., Kitcher, K.J., 1979. The geomorphology of offshore sand bars on the north coast of Ireland. In: Proceedings Royal Irish Academy Biological, Geological and Chemical Science. Royal Irish Academy, Dublin, pp. 1507–1521.

Coco, G., Huntley, D.A., Masselink, G., O'Hare, T.J., Pattiaratchi, C.B., 2000. Fractal behaviour in nearshore processes. In: Proceedings Coastal Engineering'00. ASCE, New York, pp. 2901–2913.

Froidefond, J., Gallissaires, J., Prud'Homme, R., 1990. Spatial variations in sinusoidal wave energy on a crescentic nearshore bar; application to the Cap-Ferret coast, France. Journal of Coastal Research 6, 927–942.

Homma, M., Sonu, C.J., 1962. Rhythmic pattern of longshore bars related to sediment characteristics. In: Proceedings Coastal Engineering'62. ASCE, New York, pp. 834–847.

Horel, J.D., 1984. Complex principal component analysis: theory and examples. Journal of Climate and Applied Meteorology 23, 1660–1673.

Komar, P.D., 1998. Beach Processes and Sedimentation. Prentice-Hall, New Jersey.

Liang, G., Seymour, R.J., 1991. Complex principal component analysis of wave-like sand motions. In: Proceedings Coastal Sediments'91. ASCE, New York, pp. 2175–2186.

Liang, G., White, T.E., Seymour, R.J., 1992. Complex principal component analysis of seasonal variation in nearshore bathymetry. In: Proceedings Coastal Engineering'92. ASCE, New York, pp. 2242–2250.

Lippmann, T.C., Holman, R.A., 1990. The spatial and temporal variability of sand bar morphology. Journal of Geophysical Research 95, 11,575–11,590.

Merrifield, M.A., Guza, R.T., 1990. Detecting propagating signals with complex emperical orthogonal functions: a cautionary note. Journal of Physical Oceanography 20, 1628–1633.

Nafaa, M.G., Omran, E.F., 1993. Beach and nearshore features along the dissiptive coastline of the Nile Delta, Egypt. Journal of Coastal Research 9, 423–433.

Ranasinghe, R., Symonds, G., Holman, R., 1999. Quantitative characterisation of rip dynamics via video imaging. In: Proceedings Coastal Sediments'99. ASCE, New York, pp. 987–1002.

Rasmusson, E.M., Arkin, P.A., Chen, W., 1981. Biennial variations in surface temperature over the United States as revealed by singular decomposition. Monthly Weather Review 109, 587–598.

Ruessink, B.G., 1992. The nearshore morphology of Terschelling (1965–1991). Technical Report R 92-11, Institute for Marine and Atmospheric Research Utrecht.

Ruessink, B.G., van Enckevort, I.M.J., Kingston, K.S., Davidson, M.A., 2000. Analysis of observed two- and three-dimensional nearshore bar behaviour. Marine Geology 169, 161–183.

Sallenger, A.H., Holman, R.A., Birkemeier, W.A., 1985. Storm induced response of a nearshore bar system. Marine Geology 64, 237–257.

Short, A.D., 1985. Rip-current type, spacing and persistence, Narrabean beach, Australia. Marine Geology 65, 47–71.

Short, A.D., 1992. Beach systems of the central Netherlands coast: processes, morphology and structural impacts in a storm driven multi-bar system. Marine Geology 107, 103–137.

Sonu, C.J., Russell, R.J., 1966. Topographic changes in the surf zone profile. In: Proceedings Coastal Engineering'66. ASCE, New York, pp. 502–524.

Southgate, H.N., Beltran, L.M., 1996. Self-organisational processes in beach morphology. In: Proceedings of the International Conference on Physics of Estuaries and Coastal Seas, Balkema.

Thornton, E.B., Guza, R.T., 1982. Energy saturation and phase speeds measured on a natural beach. Journal of Geophysical Research 87, 9499–9508.

Van Enckevort, I.M.J., 2001. Daily to yearly nearshore bar behaviour. Ph.D. Thesis, Utrecht University.

Van Enckevort, I.M.J., Ruessink, B.G., 2001. Alongshore uniform and nonuniform bar crest change. In: Proceedings Coastal Dynamics'01. ASCE, New York, pp. 656–665.

Van Enckevort, I.M.J., Ruessink, B.G., 2003. Video observations of nearshore bar behaviour. Part 1: alongshore uniform variability. Continental Shelf Research 23, 501–512.

Von Storch, H., Zwiers, F.W., 1999. Statistical Analysis in Climate Research. Cambridge University Press, Cambridge.

Wijnberg, K.M., 1995. Morphological behaviour of a barred coast over a period of decades. Ph.D. Thesis, Utrecht University.

Wijnberg, K.M., Terwindt, J.H.J., 1995. Extracting decadal morphological behaviour from high-resolution, long-term bathymetric surveys along the Holland coast using eigenfunction analysis. Marine Geology 126, 301–330.

Winant, C.D., Inman, D.L., Nordstrom, C.E., 1975. Description of seasonal beach changes using empirical eigenfunctions. Journal of Geophysical Research 80, 1979–1986.

Wolf, F.C.J., 1994. The response of a barred coast to a sequence of storms. In: Proceedings Coastal Dynamics'94. ASCE, New York, pp. 44–58.

Wright, L.D., Short, A.D., 1984. Morphodynamic variability of surf zones and beaches: a synthesis. Marine Geology 56, 93–118.

Wright, L.D., Short, A.D., Green, M.O., 1985. Short-term changes in the morphodynamic states of beaches and surf zones: an empirical predictive model. Marine Geology 62, 339–364.